Biomedicine & Pharmacotherapy 144 (2021) 112358

Contents lists available at ScienceDirect

Biomedicine & Pharmacotherapy

journal homepage: www.elsevier.com/locate/biopha

Sanguinarine mediated apoptosis in Non-Small Cell Lung Cancer via generation of reactive oxygen species and suppression of JAK/STAT pathway

Kirti.S. Prabhu [a,1], Ajaz A. Bhat [b,1], Kodappully S. Siveen [a], Shilpa Kuttikrishnan [a], Syed Shadab Raza [c], Thesni Raheed [a], Anh Jochebeth [d], Abdul Q. Khan [a], M.Zafar Chawdhery [e], Mohammad Haris [b,f], Michal Kulinski [a], Said Dermime [g], Martin Steinhoff [a,d,h,i], Shahab Uddin [a,d,f,*]

[a] Translational Research Institute, Academic Health System, Hamad Medical Corporation, Doha, Qatar
[b] Molecular and Metabolic Imaging Laboratory, Cancer Research Department, Sidra Medicine, Qatar
[c] Department of Stem Cell Biology and Regenerative Medicine, Era University, Lucknow 226003, India
[d] Department of Dermatology and Venereology, Hamad Medical Corporation, Doha, Qatar
[e] Surgery Department, St. Anthony's Hospital, Surrey SM3 9DW, UK
[f] Laboratory Animal Research Center, Qatar University, Doha, Qatar
[g] National Center for Cancer Care and Research, Hamad Medical Corporation, Doha, Qatar
[h] Department of Dermatology, Weill Cornell Medicine, Qatar Foundation, Education City, Doha, Qatar
[i] Department of Medicine, Weill Cornell Medicine, New York, NY, USA

ARTICLE INFO

Keywords:
Apoptosis
Antiproliferative
Alkaloids
Antioxidants
Cancer stem cells
Sanguinarine
ROS
STAT3

ABSTRACT

Effective treatment of lung cancer remains a significant clinical challenge due to its multidrug resistance and side effects of the current treatment options. The high mortality associated with this malignancy indicates the need for new therapeutic interventions with fewer side effects. Natural compounds offer various benefits such as easy access, minimal side effects, and multi-molecular targets and thus, can prove useful in treating lung cancer. Sanguinarine (SNG), a natural compound, possesses favorable therapeutic potential against a variety of cancers. Here, we examined the underlying molecular mechanisms of SNG in Non-Small Cell Lung Cancer (NSCLC) cells. SNG suppressed cell growth and induced apoptosis via downregulation of the constitutively active JAK/STAT pathway in all the NSCLC cell lines. siRNA silencing of STAT3 in NSCLC cells further confirmed the involvement of the JAK/STAT signaling cascade. SNG treatment increased Bax/Bcl-2 ratio, which contributed to a leaky mitochondrial membrane leading to cytochrome c release accompanied by caspase activation. In addition, we established the antitumor effects of SNG through reactive oxygen species (ROS) production, as inhibiting ROS production prevented the apoptosis-inducing potential of SNG. In vivo xenograft tumor model further validated our in vitro findings. Overall, our study investigated the molecular mechanisms by which SNG induces apoptosis in NSCLC, providing avenues for developing novel natural compound-based cancer therapies.

1. Introduction

Lung cancer is one of the leading causes of cancer death, accounting for 1.4 million deaths per year. Non-Small Cell Lung Cancer (NSCLC), a subtype of lung cancer, accounts for nearly 80–85% of cases [1,2]. Surgical resection at the earlier stage and chemotherapy, radiotherapy, targeted therapy, etc., at the advanced stage, is the preferred mode of treatment with a 5-year survival rate of about 15% [3]. Significant adverse effects, high cytotoxicity, and therapeutic resistance limit these targeted therapies' long-term beneficial effects [3]. The search for newer therapeutic options against NSCLC with fewer side effects continues. Herbal drugs, alone or combined with chemotherapeutic agents, are preferred due to their higher potency with fewer side effects [4].

Many medicinal plants have anticancer properties due to secondary

* Corresponding author at: Translational Research Institute, Academic Health System, Hamad Medical Corporation, Doha, Qatar.
E-mail address: SKhan34@hamad.qa (S. Uddin).
[1] Joint first authors

https://doi.org/10.1016/j.biopha.2021.112358
Received 8 August 2021; Received in revised form 8 October 2021; Accepted 19 October 2021
Available online 28 October 2021

metabolites synthesized from various phytochemical compounds such as alkaloids, flavonoids, terpenoids, etc. Such metabolites can sensitize cancer cells and cancer stem cells (CSCs) to chemotherapeutic agents by targeting multiple signaling pathways and modulating stemness properties [5]. One such medicinal plant product, the benzo phenanthridine alkaloid Sanguinarine (SNG), is isolated from the species Sanguinaria canadensis and Fumaria [6]. Several pre-clinical studies utilizing in vitro and in vivo models have previously verified the role of SNG in the treatment of a wide range of human cancers [7–15]. These studies indicated the inherent ability of SNG as a potentially interesting therapeutic candidate for cancer treatment [16,17]. In addition to many other causes, inflammation is a critical component of tumor growth and is implicated in all stages of tumorigenesis. It's becoming clear that the inflammatory tumor microenvironment (TME), which consists of cancer cells and stromal and inflammatory cells in the surrounding area, is a critical player in the neoplastic phase, promoting proliferation, survival, and migration. TME cells are extremely plastic, regularly modifying their phenotypic and functional characteristics [18]. NF-κB, a pro-inflammatory transcription factor and a key activator of inflammation, support the growth and proliferation of cancer cells and various other physiological processes like invasion, migration, metastasis, etc. NF-κB is also documented to play a significant role in regulating expressions of various inflammatory genes, which play a pivotal role in TME [19]. For instance, IL-6 supports the progression and development of colorectal cancer cells by regulating both local and systemic inflammation and the process of angiogenesis[20]. Besides, IL-6 is also an activator of STAT3 signaling that blocks apoptosis of cancer cells during the inflammatory process, thereby keeping them alive in toxic environments [21]. SNG, a natural compound, has been reported to have anti-inflammatory properties. It was observed that SNG suppressed the proliferation of A549 cells and thereby promoted apoptosis via regulating the exosomes that suppressed the NF-κB pathway in THP-1 cells [21]. SNG successfully inhibited MAPK activation, altering inflammatory mediator synthesis and release, suggesting its potential role as an anti-inflammatory agent [22,23]. We and others have demonstrated SNG's ability to inhibit IL6 secretion, thereby controlling the process of STAT3 activation [24]. In addition, SNG has also been widely reported to be used in dental products such as toothpaste and mouthwash to treat gingivitis and other inflammatory conditions[25]. In the present study, we explored the anticancer potential of SNG in NSCLC cells and in tumor xenograft model to decipher the signaling pathways involved therein.

2. Materials and methods

2.1. Reagents and antibodies

Sanguinarine chloride (Tocris, Cat. No. 2302), Cell Counting Kit-8 (Sigma Aldrich, Cat. No. 96992–100TESTS-F), and N-acetylcysteine (NAC) (Sigma Aldrich, Cat. No. A9165). z-VAD-FMK was purchased from Tocris, Cat. No. 2163). Antibodies against caspase-9 (Cat. No. 9508), Bcl2 (Cat. No. 15071), phospho-STAT3 Tyr705- Cat. No. 9145, phospho-STAT3 Ser727- Cat. No. 9134, STAT3 Cat. No.12640, cleaved caspase-3 Cat. No. 9661, caspase-3 Cat. No. 9662, Bax (Cat. No.5023), Cytochrome c (Cat. No.12963), Tubulin (Cat. No.2144), GAPDH (Cat. No.5174), PARP (Cat. No.9542) CLEAVED CASPASE 8 (Cat. No.9496), phospho-jak2 (Cat. No.3776), JAK2(Cat. No.3230), PH2AX(Cat. No.9718), phsopho-Src Tyr416 (Cat. No. 6943) and Src (Cat. No. 2108) were purchased from Cell Signaling Technologies (Beverly, USA). FITC Annexin V apoptosis detection kit I, Apo-Direct kit, Fixation/Permeabilization solution kit, BD MitoScreen (JC-1), BV421 mouse anti-γH2AX (pS139), PE rabbit anti-active caspase-3, and Alexa Fluor 700 mouse anti-cleaved PARP (Asp214) antibodies were purchased from BD Biosciences (San Jose, USA). CellROXGreen and ThiolTracker Violet were purchased from Invitrogen (Massachusetts, USA). RPMI 1640 (Cat. No. 11875–093), fetal bovine serum (FBS) (Cat. No. 10082–147), Penicillin Streptomycin (PenStrep) (Cat. No.15140122) were purchased from Life Technologies (California, USA). CytoSelect 96-well cell transformation kit was purchased from Cell Biolab Cat. No CBA-130 and Comet assay kit (Cat No ADI-900–166) from Enzo Life Sciences. Bio-Plex Pro™ Human Cytokine 27-plex Assay (Cat. No. M500KCAF0Y).

2.2. Cell culture condition

NCI-H-1975 and HCC-827 were procured from ATCC and cultured in RPMI 1640 culture medium supplemented with 10% (v/v) fetal bovine serum and 1% penicillin-streptomycin, maintained at 37 °C, in a humidified atmosphere supported with 5% CO_2. Normal lung cells LL24 was obtained from ATCC and cultured in McCoy's 5a culture medium as per ATCC instructions.

2.3. Cell viability assay

To evaluate the effect of SNG on cell viability, LL24 (normal lung fibroblast), NCI-H-1975 and HCC-827 cells were seeded separately at a density of 1×10^4 cells per well in a 96-well plate and were treated with and without SNG for 24 h. At the end of the experimental time point, the CCK-8 solution was added as per manufacturer protocol, and plates were read at 450 nm (absorbance) and plotted as percentcell viability [26].

2.4. Annexin V/propidium iodide dual staining and cell cycle analysis

NCI-H-1975 and HCC-827 cells were exposed to SNG treatment for 24 h. At the end of treatment, cells were washed with PBS and stained with either Hoechst 33342 or fluorescein-conjugated Annexin V/Propidium iodide separately and subjected to flow cytometry using BD LSRFortessa analyzer (BD Biosciences) to analyze the cell cycle fractions or to quantify the number of cells that have undergone apoptosis or necrosis respectively [27,28].

2.5. Western blotting

Lysates of SNG -treated NSCLC cells were prepared using 2 × Laemmli buffer, and for protein quantification, ND-1000 (NanoDrop Technologies, Thermo Scientific, United States) was used. After quantifying the lysates, the reducing agent (Beta-mercaptoethanol) was added, and cell lysates were resolved using SDS–PAGE. After resolving, they were transferred onto polyvinylidene difluoride (PVDF) membrane (Immobilon, Millipore, Billerica, MA, United States). PVDF membranes were later probed with antibodies separately and developed using ChemiDoc System (Amersham, Bio-Rad, United States) [26].

2.6. Mitochondrial membrane potential measurement

NCI-H-1975 and HCC-827 cells after treatment with SNG for 24 h were harvested and centrifuged. The cell pellet obtained after centrifugation was suspended in the assay buffer provided with the kit. Upon adding MitoPotential dye working solution to the assay buffer containing cell suspension, they were incubated at 37 °C for 20 min. The Muse MitoPotential 7-AAD dye was added to the cell suspension and incubated for 5 min. Change in mitochondrial membrane potential was assessed using Muse Cell Analyzer [29].

2.7. Colony formation assay

Colony formation assay was conducted to examine the anchorage-independent growth of NCI-H-1975 and HCC-827 cells following SNG treatment using CytoSelect 96-well cell transformation assay protocol [24]. Briefly, both NSCLC cell lines were treated with increasing doses of SNG (0.5, 1, 2, and 4 μM) and seeded at a density of 4×10^5 cell/ml into a 0.4% top agar layer poured over 0.6% lower agar layer and incubated for 11 days at 37° and 5% CO_2 and then colonies formed were observed using EVOS FLC Cell Imaging System (Invitrogen, Thermo Fisher

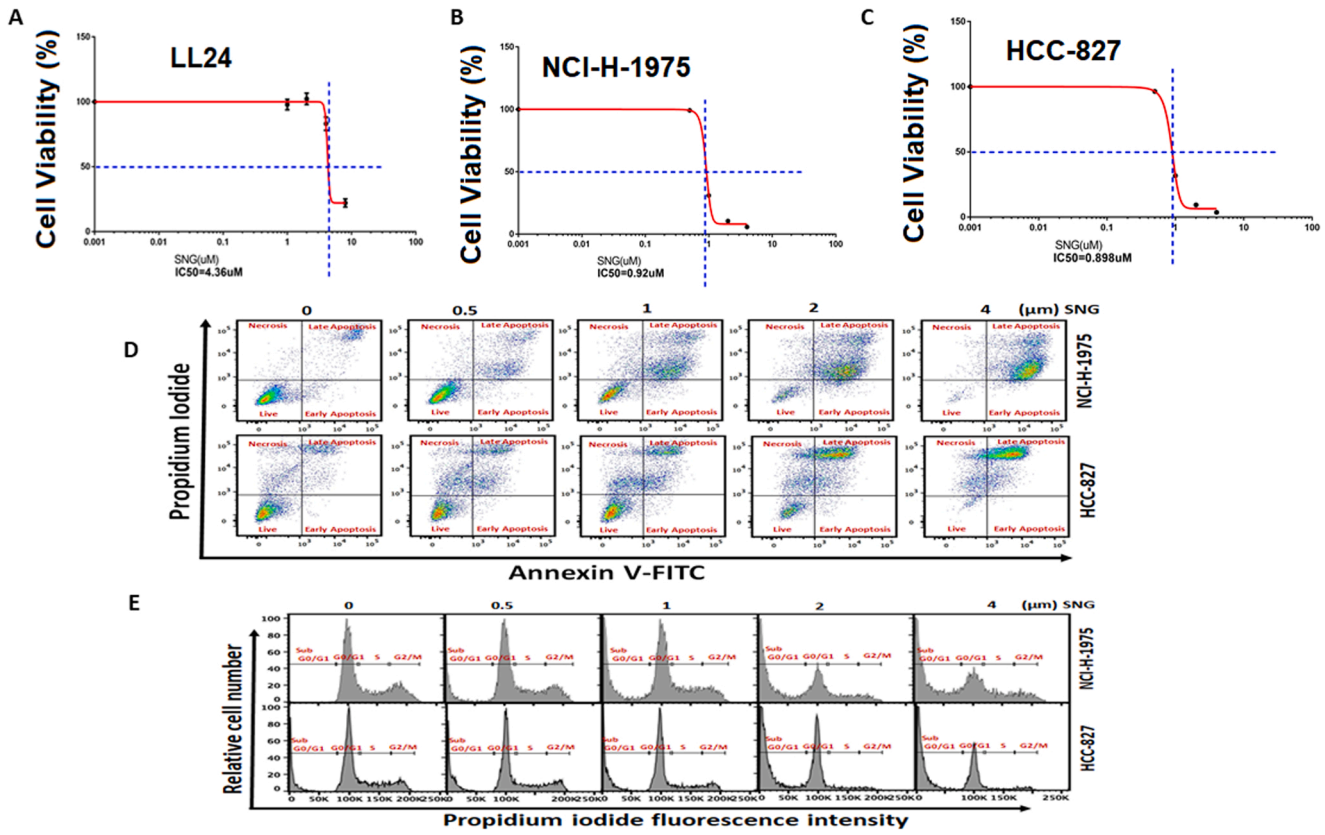

Fig. 1. Effect of SNG on cell proliferation, apoptosis, and cell cycle progression in NSCLC and cells. (A,B,C) SNG inhibits the growth of NSCLC cells. NCI-H-1975, HCC-827 cells, and a normal lung fibroblast cell line (LL24) were treated with increasing doses of SNG for 24 h, and cell proliferation assays were performed using CCK8 as mentioned under Materials and Methods. GraphPad Prism 7.01 (GraphPad Software, Inc.) was employed to compute nonlinear regression and the half-maximal inhibitory concentration 50% (IC50). (D) SNG induces apoptosis. NCI-H-1975 and HCC-827 cells were treated with increasing doses of SNG for 24 h followed by staining with fluorescein-conjugated annexin-V PI at the end of the specified time point. The percentage of apoptotic cells was analyzed by flow cytometry. (E) Effect of SNG on cell cycle progression. NCI-H-1975 and HCC-827 cells were treated with SNG with increasing doses for 24 h. After that, the cells were stained with Hoechst 33342 and analyzed for DNA content by flow cytometry. The graph displays the mean ± SD of three independent experiments. * $P < 0.05$, ** $P < 0.01$, *** $P < 0.001$.

Scientific).

2.8. Comet assay

Comet assay was performed using a comet SCGE assay kit obtained from Enzo life sciences. Briefly, after treatment of NSCLC cells with SNG for 24 h, cells at a ratio of 1:10 were mixed with low melting agarose, and 75 μL of the mixture was transferred on the comet slides and kept in the dark for 10 min. At the end of 10 min, slides were immersed first in lysis solution followed by in alkaline solution and finally into 1X TBE buffer. The slide was then moved onto a horizontal gel electrophoresis apparatus with a power supply of 1 volt per cm. Once the electrophoresis process was completed, the slides were dipped in 70% ethanol and air-dried. The diluted CYGREEN® nucleic acid dye (100 μL) was added to each slide and stained in the dark for 30 min. The slides were dried and visualized using fluorescence microscopy[24].

2.9. Release of cytochrome c assay

Following treatment of NCI-H-1975 and HCC-827 cells for 24 h with SNG, cytosolic fractions were separated as mentioned earlier [30]. Briefly, cells collected after treatment were harvested and incubated on ice-cold hypotonic buffer followed by homogenization and centrifugation to separate cytosolic fraction. Around thirty microgram protein was loaded, separated by SDS-PAGE, and finally immunoblotted using anti-cytochrome c antibody [30].

2.10. Determination of mitochondrial superoxide and reactive oxygen species

After treatment with SNG, NCI-H-1975 and HCC-827 cells for 24 h, cells were washed using HBSS and stained with either MitoSOX Red Mitochondrial Superoxide Indicator (5 μM) for 20 min or with CellROX™ Green Reagent (10 μM) for 30 min at 37 °C separately, to quantify levels of mitochondrial superoxide and ROS using flow cytometry [31,32].

2.11. Reduced glutathione measurement

NSCLC cells treated with SNG for 24 h were harvested and washed with HBSS. After washing, the cells were subjected to staining with 10 μM ThiolTracker™ Violet (Invitrogen, MA, United States) in HBSS for 30 min at 37°. Cells were rewashed with HBSS and analyzed by flow cytometry (Ex: 405, Em: 525/50) to quantify the levels of reduced glutathion[33].

2.12. Gene silencing of STAT3 using small interference RNA (siRNA)

Using lipofectamine 2000 (Invitrogen), NCI-H-1975 cells were transfected with STAT3 siRNA, Cat. No. 4390824, Life Technologies, California, USA) and Control siRNA (Cat No. 1027281, Qiagen) and later lysed, probed with different antibodies described previously [34].

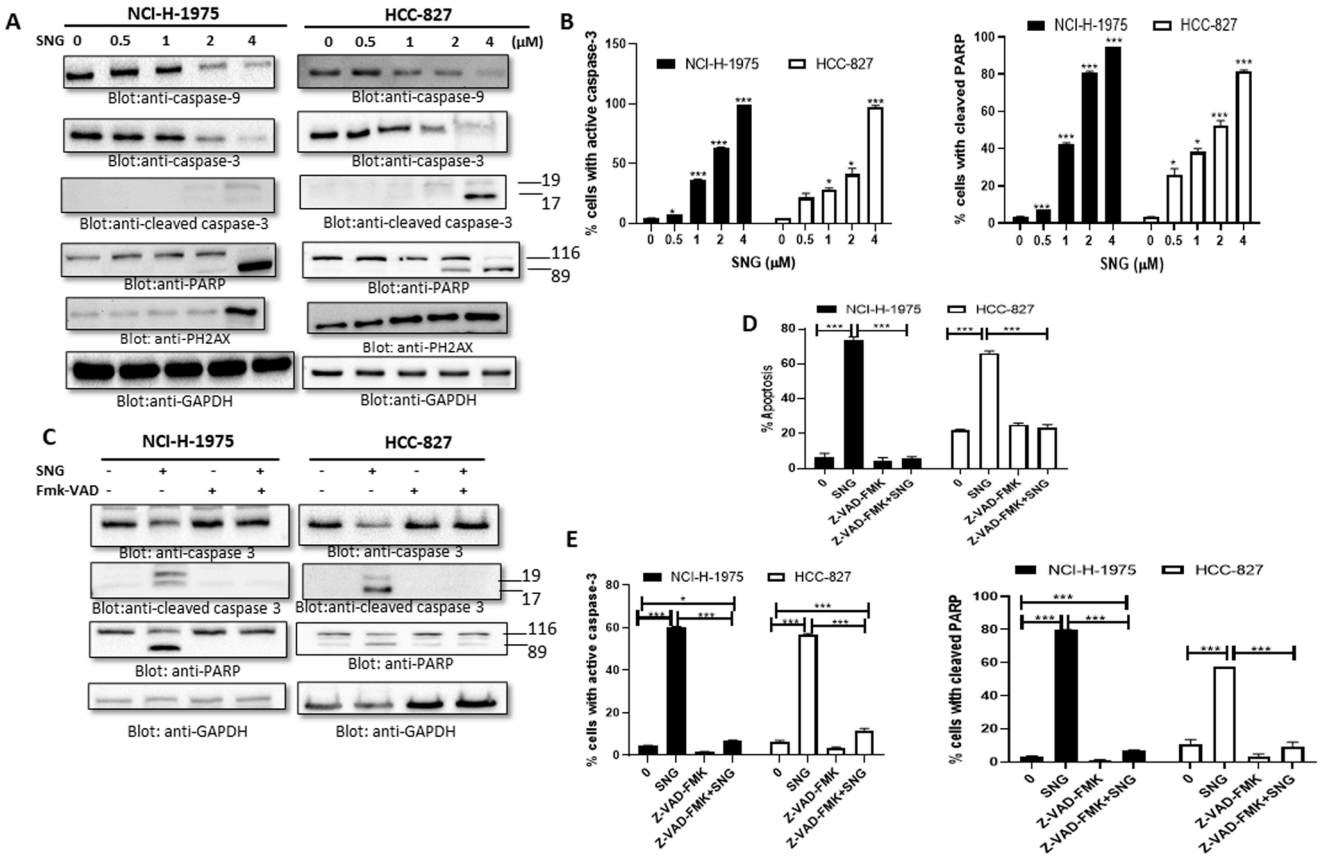

Fig. 2. SNG mediates caspase activation. To study the effect of SNG -mediated activation of caspase cascade, NCI-H-1975, and HCC-827 cells were treated with SNG in a dose-dependent manner and analyzed using (A) western blot and (B) flow cytometry for caspase-3 and PARP. The graph displays the mean ± SD of three independent experiments. * $P < 0.05$, ** $P < 0.01$, *** $P < 0.001$. Effect of z-VAD-FMK on SNG induced apoptosis. NCI-H-1975 and HCC-827 cells were pretreated with z-VAD-FMK for 1 hr followed by SNG treatment (2 μM) for 24 hr and analyzed using (C) western blot for antibodies against caspase-3, cleaved caspase-3, PARP, and GAPDH and flow cytometry for analysis of (D) % apoptosis induction (E) % Caspase-3 activation and PARP cleavage. The graph displays the mean ± SD of three independent experiments. * $P < 0.05$, ** $P < 0.01$, *** $P < 0.001$.

2.13. Cytokine analysis

NCI-H-1975 and HCC-827 cells were treated with SNG for 24 h. At the end of the experimental time point, cells were washed with PBS, trypsinized, and centrifuged at 1500 rpm for 5 min to collect the supernatant. Supernatants collected were further used for cytokine analysis. Standard curves for each cytokine were plotted using reference values supplied with the kit. Briefly, after pre-wetting the 96-well filter plate with Bio-Plex wash buffer(100 μL), around 50 μL of beads were added into each well of the 96 well plates. Next, samples obtained after treatment were incubated for 30 min with antibody-conjugated beads. Following the incubational period, detection antibodies and streptavidin-PE were added to each well for 30 min. Plates were washed to remove the unbound streptavidin-PE, the beads bound to cytokine were analyzed using Bio-Plex 200 instrument. The fluorescence intensity was evaluated using Bio-Plex Manager software (Bio-Rad) [29,35].

2.14. In vivo experiments

NCI-H1975 cells were injected subcutaneously (1×10^7 cells/site) into the flanks of donor ICR-SCID (Taconic Biosciences). 4–6 weeks later, when the tumor reached about 1000 mg, the donor mouse was euthanized, tumor collected, fragmented (~50–70 mg pieces), and transplanted unilaterally into the right flank of 10 recipients, four-five-week-old ICR-SCID female mice. One week after transplantation and once tumors were palpable, mice were randomized, separated, and ear-tagged into two groups, each with five mice. Group 1: Untreated. Group 2: treated with SNG in 3% DMSO + 97% PBS orally at 10 mg/kg QOD for 3 weeks. During treatments, mice were followed daily, and tumor measurements were recorded using a caliper and calculated using the formula LXW2 /2 to confirm the size. All mice were euthanized at the end of the experiment, and their tumors were collected for experimental analysis. The study was approved by the Institutional Animal Care and Use Committee of Wayne State University, #: 18–12–0887, and was carried out in compliance with regulations on the ethical treatment of animals.

2.15. Statistical analysis

Data were expressed as mean ± standard deviation (S.D.) and analyzed using paired student's *t*-test. Graph pad prism was used for statistical analysis and figure generation. * $P \leq 0.05$, * * $P \leq 0.001$ were considered statistically significant [36].

3. Results

3.1. SNG inhibits cell growth, causes cellular DNA damage and induces apoptosis in NSCLC cells

To evaluate cellular damage induced by SNG, NCI-H-1975 and HCC-827 cells were treated with different concentrations of SNG for 24 h. A normal fibroblast lung cell line (LL24) was also treated with SNG to confirm that SNG-mediated toxicity is specific to cancer cells. Interestingly, SNG demonstrated considerable growth inhibition against NCI-H-1975 and HCC-827 cells, as evident from their IC50 of 0.92 and 0.898, respectively, whereas LL24 demonstrated IC50 of 4.36 μM, which is

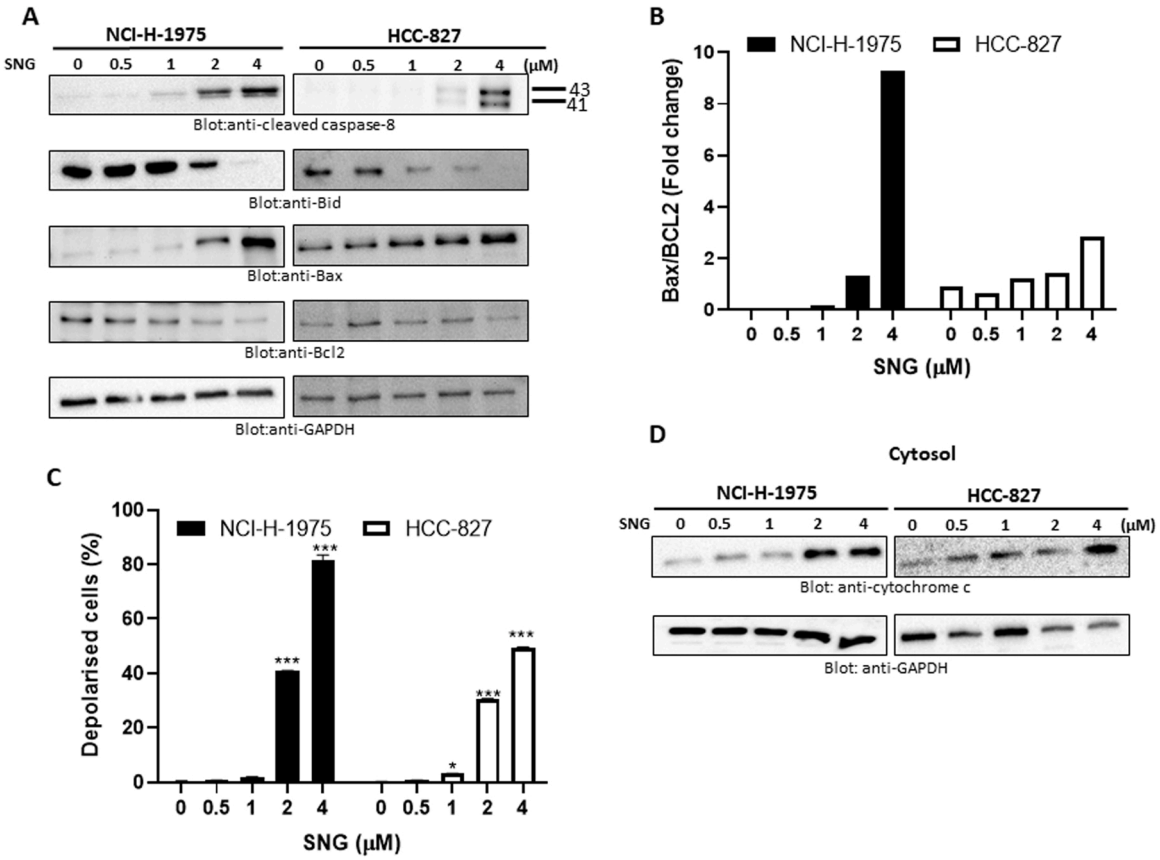

Fig. 3. SNG mediates mitochondrial signaling pathways in NSCLC cells. (A) SNG induces the activation of caspase 8 and Bid in lung cancer cell lines. NCI-H-1975 and HCC-827 cells were treated with increasing doses of SNG for 24 h, and after that, cells were lysed and immunoblotted with antibodies against cleaved caspase 8, Bid, Bax, Bcl-2, and GAPDH. (B) Effect of SNG on the Bax/Bcl-2 ratio. Data obtained from immunoblot analysis of Bax and Bcl-2 in NCI-H-1975 and HCC-827 were used to evaluate effects on Bax/Bcl-2 ratio. Densitometric analysis of Bax and Bcl-2 bands was performed using AlphaImager Software (San Leandro, CA, USA), and data (relative density normalized to GAPDH) were plotted as Bax/Bcl-2 ratio. (C) SNG treatment causes loss of mitochondrial membrane potential in NSCLC cells. NCI-H-1975 and HCC-827 cells were exposed to treatment with SNG for 24 h and analyzed by Muse analyzer. The dose-dependent loss of MMP in NCI-H-1975 and HCC-827 cells were quantified and represented as a bar graph. The graph displays the mean ± SD of three independent experiments (* $P < 0.05$, ** $P < 0.01$, and *** $P < 0.001$). (D) SNG induces the release of cytochrome c in NSCLC cells. NCI-H-1975 and HCC-827 cells were treated with increasing doses of SNG for 24 h. Proteins from cytoplasmic fractions were immunoblotted with antibodies against cytochrome c and GAPDH.

significantly higher, thus confirming the specificity of SNG mediated effects (Fig. 1A-C). SNG also inhibited colony-forming ability and displayed a significant increase in the percentage of total apoptotic phase from 19% to 97% and 18–92% in NCI-H-1975 and HCC-827 cells, respectively(Fig. 1D, Supplementary Fig. S1A,B). Cell growth and inhibition are known to be tightly regulated by cell cycle mechanisms [37]. We observed the predominance of cells in the sub-G0/G1 phase with an exponential decrease in the percentage of S-phase cell population in both cell lines following SNG treatment (Fig. 1E), further signifying that SNG triggers apoptosis. These results are thus highly suggestive of apoptosis-mediated suppression of cell growth by SNG.

Caspases are the primary drivers of apoptosis and are categorized as the initiator (such as pro-caspase-9, which activates executioner caspases) and executor (such as pro-caspase-3, which on activation gets cleaved and executes a process of apoptosis) caspases [38]. Treatment of NSCLC with SNG resulted in a decline in the expression levels of pro-caspase-9 and pro-caspase-3, coupled with an increase in the cleaved form of caspase-3 as analyzed using western blot, indicating activation of caspases in NSCLC cells. Moreover, a dose-dependent increase in the band intensity of cleaved PARP and PH2AX, markers for DNA double-strand breaks, as well as DNA fragmentation was observed (Fig. 2A, Supplementary Fig. S2). Flow cytometry data also supported the findings described above (Fig. 2B). To further confirm the role of caspase in SNG-mediated apoptosis, NCI-H-1975 and HCC-827 cells were pretreated for 1 h with z-VAD-FMK, a membrane-permeable, and irreversible pan-caspase inhibitor. SNG mediated increase in sub-G0/G1 fraction and apoptosis was abolished by z-VAD-FMK pretreatment. SNG-induced caspase activation and PARP cleavage was also nullified by z-VAD-FMK as shown in western blot analysis, indicating the caspase involvement in SNG-mediated apoptosis. (Fig. 2C-E, Supplementary Fig. S3A,B).

3.2. *SNG modulated expression levels of pro-apoptotic and anti-apoptotic molecules and induced mitochondria-mediated cell death in NSCLC cells*

Caspase-8 is implicated in apoptosis [39], and to investigate this notion, we treated NCI-H-1975 and HCC-827 cells with SNG for 24 h. Treatment with SNG induced caspase-8 activation and activated caspase-8 is known to cleave bid and cleaved bid gets translocated into mitochondria and regulates Bcl-2 family members, Bax and Bcl-2, which plays a significant role in controlling the process of apoptosis [40]. Pro-apoptotic molecule Bax supports apoptosis, while Bcl-2 interferes with this process causing imbalance and inducing resistance to chemo and radiation therapy [41–43]. Following 24 h SNG treatment, a dose-dependent decreased- Bcl-2 and increased Bax expression was exhibited in both the cell lines (Fig. 3A). Densitometric analysis revealed an increased Bax/Bcl-2 ratio suggesting the involvement of mitochondrial-mediated pathway in the apoptotic process (Fig. 3B).

The ability of SNG to induce mitochondrial membrane depolarization was examined using flow cytometry. Treatment of NCI-H-1975 and

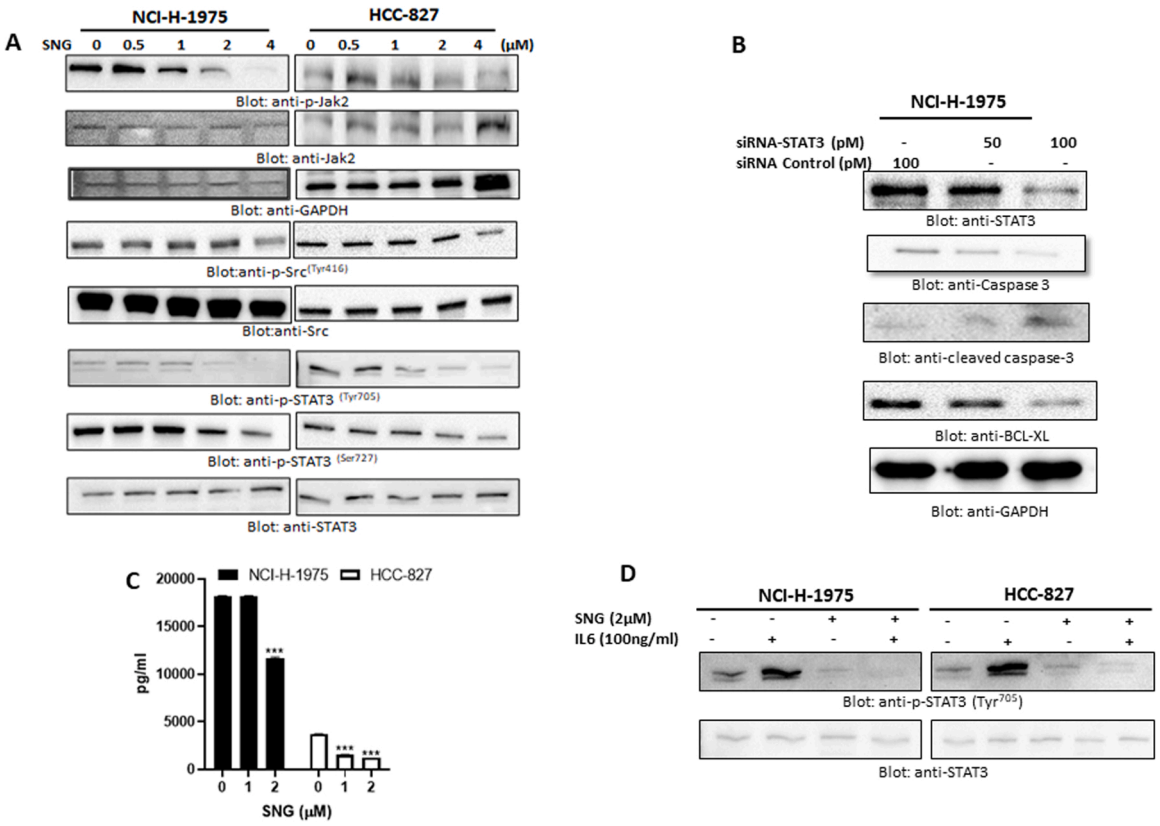

Fig. 4. SNG downregulates constitutively activated JAK/STAT3 signaling pathway and IL6 mediated STAT3 activation in NCI-H-1975 and HCC-827 cellS (A). After 24 h of SNG treatment, NCI-H-1975 and HCC-827 cells were lysed, and western blotting was performed for antibodies against p-Jak2, Jak2, GAPDH, p-Src, Src, p-STAT3 (Try705 and ser727), and STAT3. (B) siRNA knockdown of STAT3. NCI-H-1975 were transfected with control (100 pM) and STAT3 siRNA (50 and 100 pM). Cells were lysed and separated, transferred on the PVDF membrane, and immunoblotted with antibodies against STAT3, Bcl-xL, caspase-3, cleaved caspase-3 and HSP60. (C) SNG inhibits IL 6 secretion in NCI-H-1975 and HCC-827 cells. The cells mentioned above were exposed to SNG for 24 h, as indicated. Using supernatant from the treated and untreated group, levels of IL 6 were determined using multiplex biometric ELISA-based immunoassay. (D) SNG inhibits IL6-induced STAT3 activation. NCI-H-1975 and HCC-827 cells were pretreated with 2.0 μM SNG for 1 h and then stimulated with IL6 (100 μg/ml). At the end of the treatment, cells were lysed and immunoblotted against p-STAT3 (Try705) and STAT3(ser727).

HCC-827 with SNG for 24 h resulted in the loss of mitochondrial membrane potential (Fig. 3C). Damage to the mitochondrial membrane causes cytochrome c release, a critical step in the apoptotic pathway [44]. To evaluate the effect of SNG on cytochrome c release from mitochondria, NCI-H-1975 and HCC-827 cells were treated with SNG for 24 h and subjected to western blot analysis. SNG treatment caused a dose-dependent increase in the expression of cytochrome c in the cytosolic fraction (Fig. 3D). Cytochrome c, thus released, is known to trigger activation of caspase cascade, a hallmark of programmed cell death [45–47].

3.3. SNG causes inactivation of JAK2/STAT3 pathway in NSCLC cells

Receptor tyrosine kinase JAK2 and Src regulate STAT3, and aberrant activation of STAT3 is linked with a poor prognosis of lung cancer [48]. We, therefore, explored the effect of SNG on constitutively activated JAK2, Src, and STAT3 in NCI-H1975 and HCC-827 cells by immunoblotting technique. SNG inhibited the phosphorylated expression of -JAK2, Src, and STAT3 (Tyr 705 and Ser 727) in a concentration-dependent manner without affecting the total levels of these proteins (Fig. 4A, Supplementary Fig. S4 A). Besides, siRNA knockdown of STAT3 supported our results wherein down-regulation of STAT3, procaspase-3, and Bcl-xl was observed in NCI-H-1975 cells. Based on these results, we conclude that targeting constitutively activated STAT3 helped inhibit cell growth and apoptosis in lung cancer cells (Fig. 4B, Supplementary Fig. S4B(A)).

3.4. SNG inhibits IL6 induced STAT3 activation

IL6 plays a crucial role in maintaining normal cell growth through STAT3 activation, and an aberrant activation results in the proliferation of cancer cells [49]. SNG treatment prevented IL6 secretion into culture media of NCI-H-1975 and HCC-827 cells measured by a Multiplexing kit described in Material and Methods (Fig. 4C). We further investigated whether SNG treatment in NCI-H-1975 and HCC-827 cells could prevent IL6 mediated STAT3 phosphorylation as STAT3 is known to be activated by IL6 [50]. As shown in Fig. 4D and Supplementary Fig. S4B(B), pretreatment of cells with SNG blocked IL6-mediated STAT3 phosphorylation, indicating that SNG can inhibit IL6 induced STAT3 activation in both the cell lines.

3.5. SNG mediated ROS generation in NSCLC cells

ROS plays an essential role in maintaining and regulating cell proliferation and differentiation in normal cells [51]. Nonetheless, increased ROS concentration leads to loss of mitochondrial membrane potential with subsequent seepage of apoptosis-inducing factors resulting in caspase activation and nuclear condensation [52]. To investigate the ability of SNG to generate ROS, NCI-H-1975 and HCC-827 cells were treated with increasing concentrations of SNG for 24 h and analyzed for ROS generation. A significant dose-dependent increase in ROS generation at both cellular and mitochondrial level was observed in both the cell lines exposed to SNG (Fig. 5A,C). In contrast, pretreatment of these cells with a ROS scavenger, N-acetyl-L-cysteine (NAC), nullified SNG

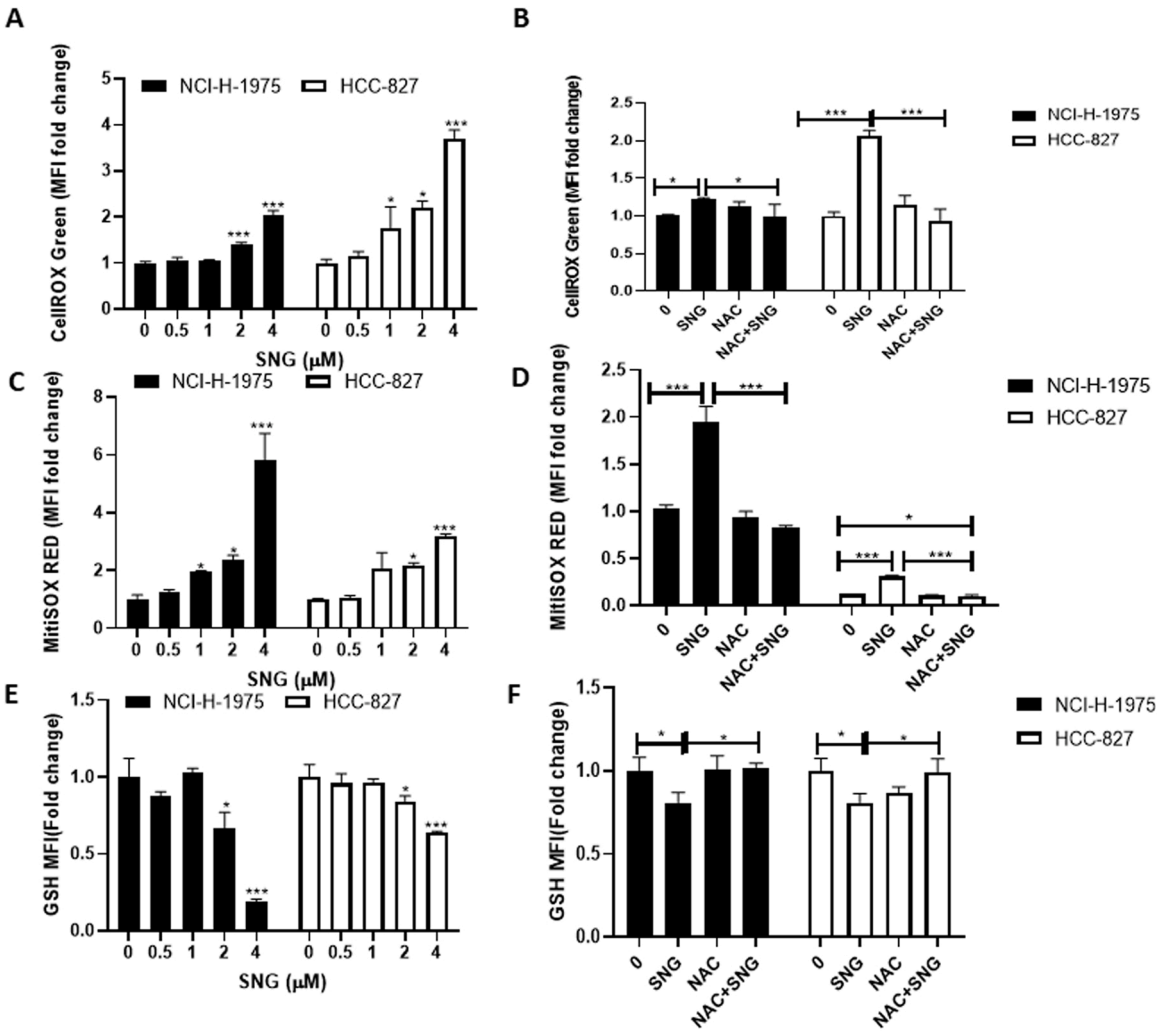

Fig. 5. SNG-mediated generation of ROS in NCI-H-1975 and HCC-827 cells. (A) NCI-H-1975 and HCC-827 cells were treated with increasing doses of SNG as indicated for 24 h. Cellrox-based flow cytometric assays were performed to quantify the levels of ROS. (B) NCI-H-1975 and HCC-827 cells were pretreated with 10 mM NAC for 2 h followed by treatment with 2 μM SNG for 24 h and level ROS determined by Cellrox-based flow cytometric assays. (c) NCI-H-1975 and HCC-827 cells were treated with increasing doses of SNG as indicated for 24 h. Mitosox-based flow cytometric assays were performed to quantify the levels of ROS. NCI-H-1975 and HCC-827 cells were pretreated with 10 mM NAC for 2 h followed by treatment with 2 μM SNG for 24 h and level ROS determined by Mitosox-based flow cytometric assays.(E) NCI-H-1975 and HCC-827 cells were treated with increasing doses of SNG as indicated for 24 h. Glutathione levels were measured using ThioTracker assay kit. (F) NCI-H-1975 and HCC-827 cells were pretreated with 10 mM NAC for 2 h followed by treatment with 2 μM SNG for 24 h and level of Glutathione was measured using ThioTracker assay kit. ROS, and GSH levels were quantified and represented as bar graphs and are expressed as mean ± SD (* $P < 0.05$, ** $P < 0.01$, *** $P < 0.001$).

mediated ROS generation (Fig. 5B, D).

3.6. SNG depletes glutathione levels in NSCLC cells

Glutathione (GSH) is an antioxidant that helps to scavenge free radicals and acts as a detoxifying agent in cells. GSH plays a dual role in cancer progression wherein higher levels support tumor progression, metastasis, and chemoresistance [24,51,53–55], and lower levels sensitize cells towards cell death [56]. To investigate the effect of SNG on GSH, we exposed both lung cancer cells to increasing doses of SNG for 24 h and analyzed GSH levels by flow cytometry. SNG-treatment displayed significant dose-dependent depletion in GSH levels (Fig. 5E). Pretreatment of cells with ROS scavenger NAC, a cysteine and GSH precursor[57] abrogated SNG induced GSH depletion in both the cell lines (Fig. 5F).

3.7. Effect of SNG on ROS generation and apoptotic cell death

As SNG-induced ROS generation, we were keen to investigate if ROS plays a role in SNG-induced cell death. As displayed in Supplementary Figs. S5A(A,B) c, S3B, SNG induced increase in the annexin V/PI staining and the level of SubG0/G1 fraction was abolished by NAC. Further, as depicted in Fig. 6A-D and Supplementary Fig. S5B, NAC pretreatment prevented SNG-induced apoptosis, caspase cascade activation, and PARP cleavage. These observations strongly suggest that SNG-induced apoptosis is mediated through ROS generation.

3.8. SNG inhibits xenograft tumor growth in ICR-SCID mice

As our in vitro observations showed promising findings, we further investigated SNG's potential in an in vivo study. NCI-H1975 cells were inoculated subcutaneously in the right flank of ICR-SCID female mice, and after one week of transplantation, SNG was given orally at 10 mg/kg QOD for 3 weeks. As depicted in Fig. 7A,B SNG administration caused

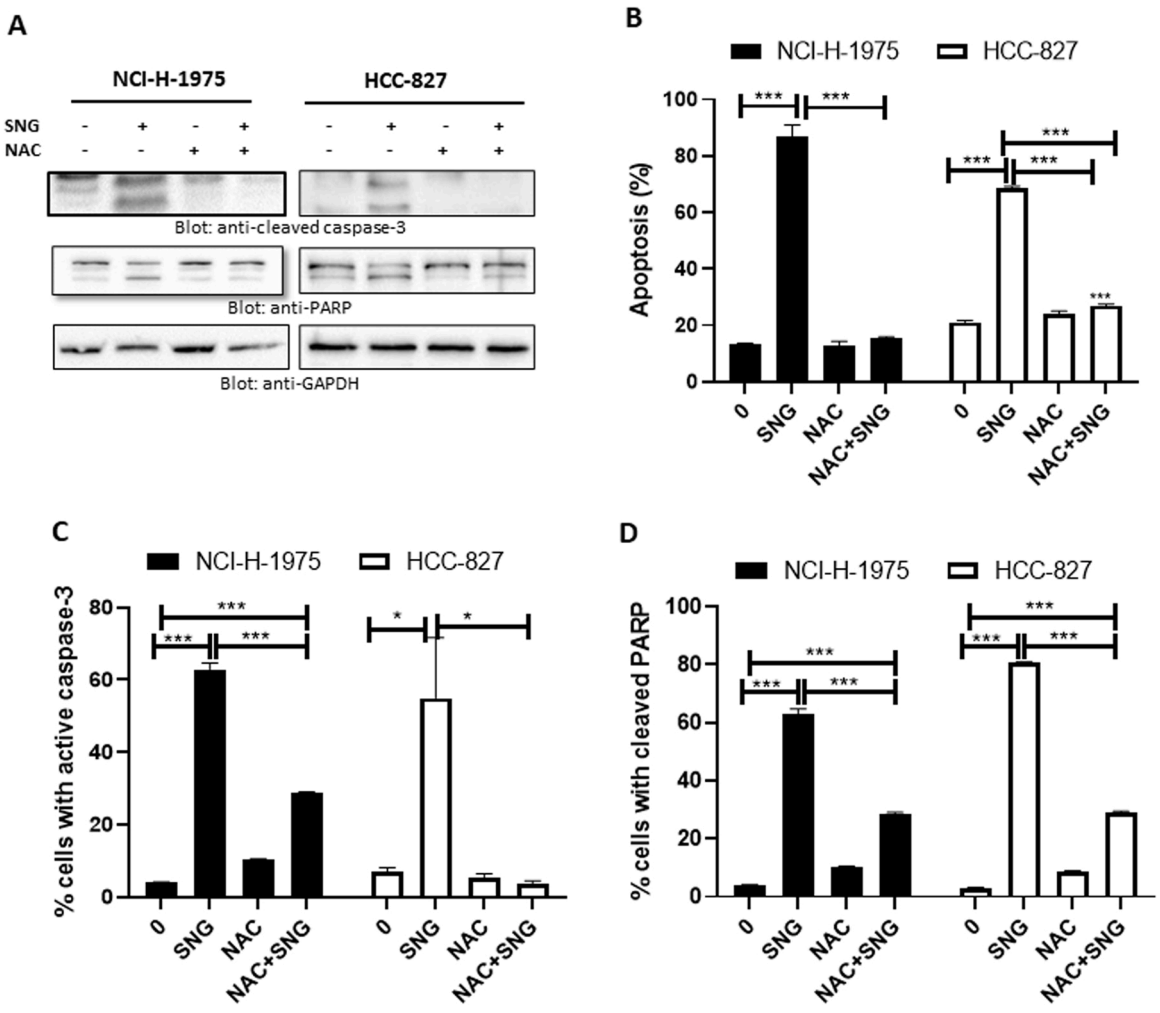

Fig. 6. SNG-induced ROS generation is involved in caspase activation and apoptotic cell death in NSCLC cells. NCI-H-1975 and HCC-827 cells were pretreated with 10 mM NAC followed by treatment with 2 μM SNG for 24 h and later subjected for analysis using (A) western blot against antibodies for cleaved caspase-3, PARP, and GAPDH and flow cytometric analysis for (B) apoptosis (C,D) Caspase-3 and PARP cleavage as described in Material and Methods. Data are expressed as mean ± SD of three independent experiments. * $P < 0.05$, * * $P < 0.01$, * ** $P < 0.001$.

significant repression in tumor growth and size compared to the control group. At the end of the treatment, tumor remnants were processed to study the effect of SNG on STAT3 phosphorylation. As shown in Fig. 7C and D, the control group displayed increased phospho and total STAT3 compared to the SNG treatment group, suggesting that SNG effectively inhibited tumor growth at the given dose. These results validate our in vitro findings and corroborate with previously published studies [58].

4. Discussion

Despite the availability of several well-known chemotherapeutic agents for lung cancer treatment, chemotherapeutic resistance remains a problem [59]. Natural compounds are considered promising candidates for cancer treatment, and we, therefore, extensively investigated the molecular mechanisms underlying the anticancer potential of SNG in NSCLC cells.

The results showed that SNG suppressed the proliferation of lung cancer cells through the activation of apoptosis. Further, our results are in concordance with previous studies, which have shown that SNG suppresses colony formation in both multiple myeloma and pre-ALL cells. [24,60]. The evidence for pro-apoptotic activity of SNG was revealed by increased annexin-V/PI positive cells, increased expression of cleaved caspase-3, and PARP cleavage following its treatment. It is well-documented that members of the Bcl-2 family play a significant role in maintaining mitochondrial membrane integrity [61]. Bax supports apoptosis while Bcl-2 interferes with this process, causing imbalance and resistance to chemotherapy., The current study showed that SNG treatment increased the Bax/Bcl-2 ratio in a concentration-dependent manner and caused significant changes in mitochondrial membrane potential. Our findings are consistent with previously published studies [24,26]. SNG treatment triggered the release of cytochrome c, followed by caspase cascade activation, thereby inducing apoptosis [24]. z-VAD-FMK, a pan-caspase inhibitor, negated SNG-mediated apoptosis and caspase activation as analyzed by western blot and flow cytometry, thus confirming caspase-mediated cell death induced by SNG.

Reactive oxygen species (ROS) are metabolic by-products known to have harmful and beneficial effects. Accumulation of ROS above threshold level leads to loss of cellular integrity and functions [7,8]. GSH is considered one of the key antioxidants due to its ability to scavenges ROS, thereby maintaining an intracellular redox state [62]. Several attempts have been made to increase intracellular ROS levels to suppress tumor growth through the inhibition of GSH. SNG treatment in NCI-H-1975 and HCC-827 cells increased both cellular and mitochondrial ROS in a dose-dependent manner, followed by depletion of GSH, suggesting ROS involvement in SNG-mediated apoptosis. To further confirm this, pretreatment of NCI-H-1975 and HCC-827 cells with ROS scavenger NAC abrogated SNG-induced caspase activation and PARP cleavage, indicating the role of SNG in ROS generation. Several other

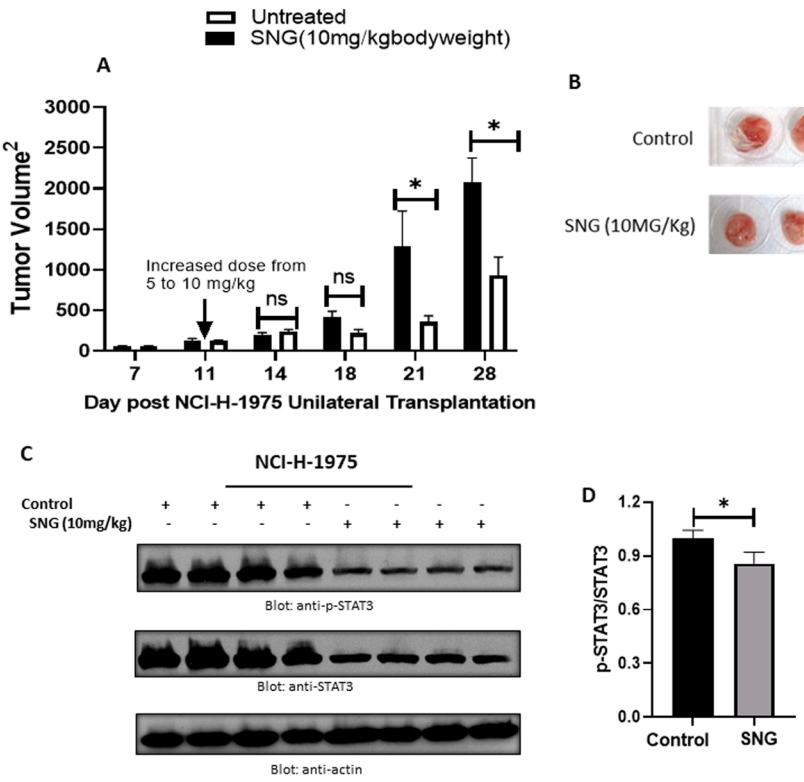

Fig. 7. SNG inhibits NCI-H-1975 xenograft tumor growth in ICR-SCID mice. Subcutaneous tumor was grown in donor mouse and then transplanted into ICR-SCID female mice and divided into treated and control groups as discussed under Materials and Methods. At the end of the study, the mice were sacrificed, and (A) excised tumors in each group were weighed and analyzed using graph pad prism software. The graph displays the mean ± SD of four independent experiments (* $P < 0.05$). (B) Excised tumors were photographed (C) lysates obtained from excised tumors were immunoblotted against p-STAT3, STAT3, and actin antibodies. (D) Densitometric analysis of p-STAT3/STAT3 expression in control and SNG treated tumors. The graph displays the mean ± SD of four independent experiments (* $P < 0.05$).

studies have also documented similar findings [24,53,60,63].

Janus kinase 1 and 2 are transducers of heteromeric receptors of IL-6 and IL-10 that activate STAT3 and regulates cellular growth, apoptosis, and autophagy [64,65]. Aberrant activation of STAT3 is associated with poor prognosis, cancer cell proliferation, and resistance to chemotherapy in lung cancer patients [65]. Activated STAT3 controls transcription of various anti-apoptotic genes, and dysregulated expression of these genes confers chemotherapeutic resistance [24]. SNG inhibited phosphorylation of JAK2, Src, STAT3 (Tyr 705 and Ser 727) thereby, preventing dimerization, nucleocytoplasmic shuttling, and transcriptional activity in NSCLC cells [66,67]. Interestingly, our data showed that STAT3 silencing using siRNA decreased the expression of STAT3, Bcl-xL, and caspase-3, resulting in inhibition of tumor growth. These findings are in concert with previously published results in solid and hematological tumors [68]. It has also been shown that IL-6/JAK/STAT3 signaling axis plays a major role in the growth and proliferation of cancer cells. Increased IL-6 levels in the serum can cause hyperactivation of STAT3 in tumors/cancer cells and correlate with poor prognosis and reduced survival rates [50]. In this study, we found decreased expression of IL-6 and phosphorylated STAT3 (Y705). We also confirmed ours in vitro findings in in vivo model. The in vivo results demonstrated that SNG treatment not only decreased tumor volume and weight but also prevented STAT3 phosphorylation, indicating that blocking transcription factors could be an effective way to treat cancer [69].

5. Conclusion

In conclusion, we demonstrated that SNG inhibited proliferation, cell cycle progression and induced apoptosis in NSCLC cells by altering the expression of STAT3. Our in vitro results are strengthened by vivo data showing STAT3 inhibition regulated the tumor progression in the treatment group. Based on the previously published studies and our results, we believe that SNG could be a promising anticancer compound. The results from this study would serve as the basis for carrying future in-depth investigations in delineating the potential of SNG in cancer treatment.

Funding

The Medical Research Centre at Hamad Medical Corporation, Qatar supported this work under the approved project number MRC 16354/16.

CrediT authorship contribution statement

Shahab Uddin: Conceptualization, Supervision, Writing – review & editing. **Kirti. S. Prabhu, Kodappully S. Siveen, Shilpa Kuttikrishnan, Ajaz A. Bhat, Abdul Q. Khan:** Investigation, Data curation, Conceptualization, Writing – original draft. **M Zafar Chawdhery, Mohammad Haris, Syed Shadab Raza, Thesni Raheed, Anh Jocobeth, Michal Kulinski, Said Dermime:** Writing – review & editing. **Martin Steinhoff**: Conceptualization, Supervision, Resources. All authors have read and agreed to the published version of the manuscript.

Conflicts of interest statement

The authors have no conflict of interest to declare.

Data availability

The data sets generated during and/or analyzed during the current study are available from the corresponding author on reasonable request.

Acknowledgments

We would like to thank Karmanos Cancer Institute, Wayne State University, Detroit, MI, to provide service for the in vivo study and Qatar National Library, Doha, Qatar, to fund this article's open access publication charge.

Appendix A. Supporting information

Supplementary data associated with this article can be found in the online version at doi:10.1016/j.biopha.2021.112358.

References

[1] S.L. Wood, M. Pernemalm, P.A. Crosbie, A.D. Whetton, Molecular histology of lung cancer: from targets to treatments, Cancer Treat. Rev. 41 (4) (2015) 361–375.
[2] M.Y. Alfaifi, Kanahia Laniflora, Methanolic extract suppressed proliferation of human Non-Small Cell Lung Cancer A549 cells, Asian Pac. J. Cancer Prev. 17 (10) (2016) 4755–4759.
[3] J. Poofery, P. Khaw-On, S. Subhawa, B. Sripanidkulchai, A. Tantraworasin, S. Saeteng, S. Siwachat, N. Lertprasertsuke, R. Banjerdpongchai, Potential of thai herbal extracts on lung cancer treatment by inducing apoptosis and synergizing chemotherapy, Molecules 25 (1) (2020).
[4] R. Kasole, H.D. Martin, J. Kimiywe, Traditional medicine and its role in the management of diabetes mellitus: “patients’ and herbalists’ perspectives”, Evid. Based Complement Altern. Med. 2019 (2019), 2835691.
[5] M.E. Ciurea, A.M. Georgescu, S.O. Purcaru, S.A. Artene, G.H. Emami, M. V. Boldeanu, D.E. Tache, A. Dricu, Cancer stem cells: biological functions and therapeutically targeting, Int. J. Mol. Sci. 15 (5) (2014) 8169–8185.
[6] S. Reagan-Shaw, J. Breur, N. Ahmad, Enhancement of UVB radiation-mediated apoptosis by sanguinarine in HaCaT human immortalized keratinocytes, Mol. Cancer Ther. 5 (2) (2006) 418–429.
[7] I.W. Achkar, F. Mraiche, R.M. Mohammad, S. Uddin, Anticancer potential of sanguinarine for various human malignancies, Future Med. Chem. 9 (9) (2017) 933–950.
[8] B.C. Jang, J.G. Park, D.K. Song, W.K. Baek, S.K. Yoo, K.H. Jung, G.Y. Park, T.Y. Lee, S.I. Suh, Sanguinarine induces apoptosis in A549 human lung cancer cells primarily via cellular glutathione depletion, Toxicol. Vitr. 23 (2) (2009) 281–287.
[9] Y.H. Choi, W.Y. Choi, S.H. Hong, S.O. Kim, G.Y. Kim, W.H. Lee, Y.H. Yoo, Anti-invasive activity of sanguinarine through modulation of tight junctions and matrix metalloproteinase activities in MDA-MB-231 human breast carcinoma cells, Chem. Biol. Interact. 179 (2–3) (2009) 185–191.
[10] S.Y. Park, M.L. Jin, Y.H. Kim, S.J. Lee, G. Park, Sanguinarine inhibits invasiveness and the MMP-9 and COX-2 expression in TPA-induced breast cancer cells by inducing HO-1 expression, Oncol. Rep. 31 (1) (2014) 497–504.
[11] T.L. Serafim, J.A. Matos, V.A. Sardao, G.C. Pereira, A.F. Branco, S.L. Pereira, D. Parke, E.L. Perkins, A.J. Moreno, J. Holy, P.J. Oliveira, Sanguinarine cytotoxicity on mouse melanoma K1735-M2 cells–nuclear vs. mitochondrial effects, Biochem. Pharmacol. 76 (11) (2008) 1459–1475.
[12] A. Burgeiro, A.C. Bento, C. Gajate, P.J. Oliveira, F. Mollinedo, Rapid human melanoma cell death induced by sanguinarine through oxidative stress, Eur. J. Pharmacol. 705 (1–3) (2013) 109–118.
[13] P. Weerasinghe, S. Hallock, S.C. Tang, A. Liepins, Role of Bcl-2 family proteins and caspase-3 in sanguinarine-induced bimodal cell death, Cell Biol. Toxicol. 17 (6) (2001) 371–381.
[14] P. Weerasinghe, S. Hallock, S.C. Tang, B. Trump, A. Liepins, Sanguinarine overcomes P-glycoprotein-mediated multidrug-resistance via induction of apoptosis and oncosis in CEM-VLB 1000 cells, Exp. Toxicol. Pathol. 58 (1) (2006) 21–30.
[15] V. Kaminskyy, O. Kulachkovskyy, R. Stoika, A decisive role of mitochondria in defining rate and intensity of apoptosis induction by different alkaloids, Toxicol. Lett. 177 (3) (2008) 168–181.
[16] A.R. Hussain, N.A. Al-Jomah, A.K. Siraj, P. Manogaran, K. Al-Hussein, J. Abubaker, L.C. Platanias, K.S. Al-Kuraya, S. Uddin, Sanguinarine-dependent induction of apoptosis in primary effusion lymphoma cells, Cancer Res. 67 (8) (2007) 3888–3897.
[17] R. Gaziano, G. Moroni, C. Bue, M.T. Miele, P. Sinibaldi-Vallebona, F. Pica, Antitumor effects of the benzophenanthridine alkaloid sanguinarine: evidence and perspectives, World J. Gastrointest. Oncol. 8 (1) (2016) 30–39.
[18] F.R. Greten, S.I. Grivennikov, Inflammation and cancer: triggers, mechanisms, and consequences, Immunity 51 (1) (2019) 27–41.
[19] Y. Yu, Y. Luo, Z. Fang, W. Teng, Y. Yu, J. Tian, P. Guo, R. Xu, J. Wu, Y. Li, Mechanism of sanguinarine in inhibiting macrophages to promote metastasis and proliferation of lung cancer via modulating the exosomes in A549 cells, Onco Targets Ther. 13 (2020) 8989–9003.
[20] G.J. Guthrie, C.S. Roxburgh, C.H. Richards, P.G. Horgan, D.C. McMillan, Circulating IL-6 concentrations link tumour necrosis and systemic and local inflammatory responses in patients undergoing resection for colorectal cancer, Br. J. Cancer 109 (1) (2013) 131–137.
[21] D.R. Hodge, E.M. Hurt, W.L. Farrar, The role of IL-6 and STAT3 in inflammation and cancer, Eur. J. Cancer 41 (16) (2005) 2502–2512.
[22] T.G. Shrihari, Dual role of inflammatory mediators in cancer, Ecancermedicalscience 11 (2017) 721.
[23] X. Niu, T. Fan, W. Li, W. Xing, H. Huang, The anti-inflammatory effects of sanguinarine and its modulation of inflammatory mediators from peritoneal macrophages, Eur. J. Pharmacol. 689 (1–3) (2012) 262–269.
[24] S. Akhtar, I.W. Achkar, K.S. Siveen, S. Kuttikrishnan, K.S. Prabhu, A.Q. Khan, E. I. Ahmed, F. Sahir, J. Jerobin, A. Raza, M. Merhi, H.M. Elsabah, R. Taha, H. E. Omri, H. Zayed, S. Dermime, M. Steinhoff, S. Uddin, Sanguinarine induces apoptosis pathway in multiple myeloma cell lines via inhibition of the JaK2/STAT3 signaling, Front. Oncol. 9 (2019) 285.
[25] V.M. Adhami, M.H. Aziz, H. Mukhtar, N. Ahmad, Activation of prodeath Bcl-2 family proteins and mitochondrial apoptosis pathway by sanguinarine in immortalized human HaCaT keratinocytes, Clin. Cancer Res. 9 (8) (2003) 3176–3182.
[26] K.S. Prabhu, K.S. Siveen, S. Kuttikrishnan, A.N. Iskandarani, A.Q. Khan, M. Merhi, H.E. Omri, S. Dermime, T. El-Elimat, N.H. Oberlies, F.Q. Alali, S. Uddin, Greensporone C, a freshwater fungal secondary metabolite induces mitochondrial-mediated apoptotic cell death in leukemic cell lines, Front. Pharmacol. 9 (2018) 720.
[27] K.S. Siveen, N. Mustafa, F. Li, R. Kannaiyan, K.S. Ahn, A.P. Kumar, W.J. Chng, G. Sethi, Thymoquinone overcomes chemoresistance and enhances the anticancer effects of bortezomib through abrogation of NF-kappaB regulated gene products in multiple myeloma xenograft mouse model, Oncotarget 5 (3) (2014) 634–648.
[28] J.A. Badmus, O.E. Ekpo, A.A. Hussein, M. Meyer, D.C. Hiss, Antiproliferative and apoptosis induction potential of the methanolic leaf extract of holarrhena floribunda (G. Don), Evid. Based Complement. Altern. Med. 2015 (2015), 756482.
[29] A. Sorice, F. Siano, F. Capone, E. Guerriero, G. Picariello, A. Budillon, G. Ciliberto, M. Paolucci, S. Costantini, M.G. Volpe, Potential anticancer effects of polyphenols from chestnut shell extracts: modulation of cell growth, and cytokinomic and metabolomic profiles, Molecules 21 (10) (2016).
[30] S. Uddin, A.R. Hussain, P.S. Manogaran, K. Al-Hussein, L.C. Platanias, M. I. Gutierrez, K.G. Bhatia, Curcumin suppresses growth and induces apoptosis in primary effusion lymphoma, Oncogene 24 (47) (2005) 7022–7030.
[31] G. Syn, D. Anderson, J.M. Blackwell, S.E. Jamieson, Toxoplasma gondii infection is associated with mitochondrial dysfunction in-vitro, Front. Cell. Infect. Microbiol. 7 (2017) 512.
[32] C. Weidner, M. Rousseau, A. Plauth, S.J. Wowro, C. Fischer, H. Abdel-Aziz, S. Sauer, Iberis amara extract induces intracellular formation of reactive oxygen species and inhibits colon cancer, PLoS One 11 (4) (2016), e0152398.
[33] C. Morzadec, M. Macoch, L. Sparfel, S. Kerdine-Romer, O. Fardel, L. Vernhet, Nrf2 expression and activity in human T lymphocytes: stimulation by T cell receptor activation and priming by inorganic arsenic and tert-butylhydroquinone, Free Radic. Biol. Med. 71 (2014) 133–145.
[34] A.Q. Khan, K.S. Siveen, K.S. Prabhu, S. Kuttikrishnan, S. Akhtar, A. Shaar, A. Raza, F. Mraiche, S. Dermime, S. Uddin, Curcumin-mediated degradation of S-phase kinase protein 2 induces cytotoxic effects in human papillomavirus-positive and negative squamous carcinoma cells, Front. Oncol. 8 (2018) 399.
[35] E. Szliszka, D. Skaba, Z.P. Czuba, W. Krol, Inhibition of inflammatory mediators by neobavaisoflavone in activated RAW264.7 macrophages, Molecules 16 (5) (2011) 3701–3712.
[36] N.H. Yim, Y.P. Jung, A. Kim, T. Kim, J.Y. Ma, Induction of apoptotic cell death by betulin in multidrug-resistant human renal carcinoma cells, Oncol. Rep. 34 (2) (2015) 1058–1064.
[37] K.L. Collins, T.J. Kelly, Effects of T antigen and replication protein A on the initiation of DNA synthesis by DNA polymerase alpha-primase, Mol. Cell Biol. 11 (4) (1991) 2108–2115.
[38] H. Chen, B. Zhou, J. Yang, X. Ma, S. Deng, Y. Huang, Y. Wen, J. Yuan, X. Yang, Essential oil derived from eupatorium adenophorum spreng. mediates anticancer effect by inhibiting STAT3 and AKT activation to induce apoptosis in hepatocellular carcinoma, Front. Pharmacol. 9 (2018) 483.
[39] S. Uddin, M. Ahmed, P. Bavi, R. El-Sayed, N. Al-Sanea, A. AbdulJabbar, L. H. Ashari, S. Alhomoud, F. Al-Dayel, A.R. Hussain, K.S. Al-Kuraya, Bortezomib (Velcade) induces p27Kip1 expression through S-phase kinase protein 2 degradation in colorectal cancer, Cancer Res. 68 (9) (2008) 3379–3388.
[40] R.J. Anto, A. Mukhopadhyay, K. Denning, B.B. Aggarwal, Curcumin (diferuloylmethane) induces apoptosis through activation of caspase-8, BID cleavage and cytochrome c release: its suppression by ectopic expression of Bcl-2 and Bcl-xl, Carcinogenesis 23 (1) (2002) 143–150.
[41] K. Thangaraj, B. Balasubramanian, S. Park, K. Natesan, W. Liu, V. Manju, Orientin induces G0/G1 cell cycle arrest and mitochondria mediated intrinsic apoptosis in human colorectal carcinoma HT29 cells, Biomolecules 9 (9) (2019).
[42] J.C. Reed, Bcl-2 and the regulation of programmed cell death, J. Cell Biol. 124 (1–2) (1994) 1–6.
[43] J.C. Martinou, R.J. Youle, Mitochondria in apoptosis: Bcl-2 family members and mitochondrial dynamics, Dev. Cell 21 (1) (2011) 92–101.
[44] Q. Zhao, X.C. Huo, F.D. Sun, R.Q. Dong, Polyphenol-rich extract of Salvia chinensis exhibits anticancer activity in different cancer cell lines, and induces cell cycle arrest at the G(0)/G(1)-phase, apoptosis and loss of mitochondrial membrane potential in pancreatic cancer cells, Mol. Med. Rep. 12 (4) (2015) 4843–4850.
[45] D. Chandra, J.W. Liu, D.G. Tang, Early mitochondrial activation and cytochrome c up-regulation during apoptosis, J. Biol. Chem. 277 (52) (2002) 50842–50854.
[46] Z. Cai, M. Lin, C. Wuchter, V. Ruppert, B. Dorken, W.D. Ludwig, L. Karawajew, Apoptotic response to homoharringtonine in human wt p53 leukemic cells is independent of reactive oxygen species generation and implicates Bax translocation, mitochondrial cytochrome c release and caspase activation, Leukemia 15 (4) (2001) 567–574.
[47] C.Y. Looi, A. Arya, F.K. Cheah, B. Muharram, K.H. Leong, K. Mohamad, W.F. Wong, N. Rai, M.R. Mustafa, Induction of apoptosis in human breast cancer cells via caspase pathway by vernodalin isolated from Centratherum anthelminticum (L.) seeds, PLoS One 8 (2) (2013), e56643.
[48] D. Harada, N. Takigawa, K. Kiura, The role of STAT3 in non-small cell lung cancer, Cancers (Basel) 6 (2) (2014) 708–722.
[49] Y. Wang, A.H. van Boxel-Dezaire, H. Cheon, J. Yang, G.R. Stark, STAT3 activation in response to IL-6 is prolonged by the binding of IL-6 receptor to EGF receptor, Proc. Natl. Acad. Sci. USA 110 (42) (2013) 16975–16980.

[50] D.E. Johnson, R.A. O'Keefe, J.R. Grandis, Targeting the IL-6/JAK/STAT3 signalling axis in cancer, Nat. Rev. Clin. Oncol. 15 (4) (2018) 234–248.
[51] D. Zhou, L. Shao, D.R. Spitz, Reactive oxygen species in normal and tumor stem cells, Adv. Cancer Res. 122 (2014) 1–67.
[52] M.J. Lee, S.H. Kao, J.E. Hunag, G.T. Sheu, C.W. Yeh, Y.C. Hseu, C.J. Wang, L. S. Hsu, Shikonin time-dependently induced necrosis or apoptosis in gastric cancer cells via generation of reactive oxygen species, Chem. Biol. Interact. 211 (2014) 44–53.
[53] K.S. Prabhu, K.S. Siveen, S. Kuttikrishnan, A. Jochebeth, T.A. Ali, N.R. Elareer, A. Iskandarani, A. Quaiyoom Khan, M. Merhi, S. Dermime, T. El-Elimat, N. H. Oberlies, F.Q. Alali, M. Steinhoff, S. Uddin, Greensporone a, a fungal secondary metabolite suppressed constitutively activated AKT via ros generation and induced apoptosis in leukemic cell lines, Biomolecules 9 (4) (2019).
[54] A. Bansal, M.C. Simon, Glutathione metabolism in cancer progression and treatment resistance, J. Cell Biol. 217 (7) (2018) 2291–2298.
[55] R. Sarangarajan, S. Meera, R. Rukkumani, P. Sankar, G. Anuradha, Antioxidants: friend or foe? Asian Pac. J. Trop. Med. 10 (12) (2017) 1111–1116.
[56] N. Traverso, R. Ricciarelli, M. Nitti, B. Marengo, A.L. Furfaro, M.A. Pronzato, U. M. Marinari, C. Domenicotti, Role of glutathione in cancer progression and chemoresistance, Oxid. Med Cell Longev. 2013 (2013), 972913.
[57] M. Halasi, M. Wang, T.S. Chavan, V. Gaponenko, N. Hay, A.L. Gartel, ROS inhibitor N-acetyl-L-cysteine antagonizes the activity of proteasome inhibitors, Biochem. J. 454 (2) (2013) 201–208.
[58] A. Ahmad, S.H. Sarkar, A. Aboukameel, S. Ali, B. Biersack, S. Seibt, Y. Li, B. Bao, D. Kong, S. Banerjee, R. Schobert, S.B. Padhye, F.H. Sarkar, Anticancer action of garcinol in vitro and in vivo is in part mediated through inhibition of STAT-3 signaling, Carcinogenesis 33 (12) (2012) 2450–2456.
[59] B. Mansoori, A. Mohammadi, S. Davudian, S. Shirjang, B. Baradaran, The different mechanisms of cancer drug resistance: a brief review, Adv. Pharm. Bull. 7 (3) (2017) 339–348.
[60] S. Kuttikrishnan, K.S. Siveen, K.S. Prabhu, A.Q. Khan, S. Akhtar, J.M. Mateo, M. Merhi, R. Taha, H.E. Omri, F. Mraiche, S. Dermime, S. Uddin, Sanguinarine suppresses growth and induces apoptosis in childhood acute lymphoblastic leukemia, Leuk. Lymphoma 60 (3) (2019) 782–794.
[61] R.J. Youle, A. Strasser, The BCL-2 protein family: opposing activities that mediate cell death, Nat. Rev. Mol. Cell Biol. 9 (1) (2008) 47–59.
[62] R. Franco, J.A. Cidlowski, Apoptosis and glutathione: beyond an antioxidant, Cell Death Differ. 16 (10) (2009) 1303–1314.
[63] S. Kuttikrishnan, K.S. Siveen, K.S. Prabhu, A.Q. Khan, E.I. Ahmed, S. Akhtar, T. A. Ali, M. Merhi, S. Dermime, M. Steinhoff, S. Uddin, Curcumin induces apoptotic cell death via inhibition of PI3-kinase/AKT pathway in B-precursor acute lymphoblastic leukemia, Front. Oncol. 9 (2019) 484.
[64] N. Losuwannarak, A. Maiuthed, N. Kitkumthorn, A. Leelahavanichkul, S. Roytrakul, P. Chanvorachote, Gigantol targets cancer stem cells and destabilizes tumors via the suppression of the PI3K/AKT and JAK/STAT pathways in ectopic lung cancer xenografts, Cancers (Basel) 11 (12) (2019).
[65] W. Cao, Y. Liu, R. Zhang, B. Zhang, T. Wang, X. Zhu, L. Mei, H. Chen, H. Zhang, P. Ming, L. Huang, Homoharringtonine induces apoptosis and inhibits STAT3 via IL-6/JAK1/STAT3 signal pathway in Gefitinib-resistant lung cancer cells, Sci. Rep. 5 (2015) 8477.
[66] J.F. Bromberg, M.H. Wrzeszczynska, G. Devgan, Y. Zhao, R.G. Pestell, C. Albanese, J.E. Darnell Jr., Stat3 as an oncogene, Cell 98 (3) (1999) 295–303.
[67] M.Z. Kamran, P. Patil, R.P. Gude, Role of STAT3 in cancer metastasis and translational advances, Biomed. Res. Int. 2013 (2013), 421821.
[68] K. Al Zaid Siddiquee, J. Turkson, STAT3 as a target for inducing apoptosis in solid and hematological tumors, Cell Res. 18 (2) (2008) 254–267.
[69] H. Zhang, J. Zhang, P.S. Venkat, C. Gu, Y. Meng, Sanguinarine exhibits potent efficacy against cervical cancer cells through inhibiting the STAT3 pathway in vitro and in vivo, Cancer Manag. Res. 11 (2019) 7557–7566.